

# Aortic Pulsatility Propagates Intracranially and Correlates with Dilated Perivascular Spaces and Small Vessel Compliance

Owen Thomas, BM, BCh, DPhil, FRCR,<sup>\*,1</sup> John Cain, MB, ChB, PhD, FRCR,<sup>\*,†,2</sup>  
Mehran Nasralla, MB, ChB,<sup>†,3</sup> and Alan Jackson, MB, ChB, PhD, FRCP, FRCR, FBIR<sup>\*,†,4</sup>

*Introduction:* To test the hypotheses that changes in the aortic pulse-wave produced by arterial stiffening are (1) propagated into cerebral small vessels, (2) associated with reduced compliance of small cerebral arterial vessels, and (3) associated with the presence of dilated perivascular spaces (PVS). *Methods:* Fifteen volunteers and 19 patients with late-onset depression (LOD) were prospectively recruited, of which 6 fulfilled the criteria for treatment-resistant depression (TRD). Aortic pulse-wave velocity (PWV) was determined using Carotid-Femoral Doppler. Pulse-wave analysis (PWA) was performed using a SphygmoCor system. White-matter lesion load and PVS were scored on established MRI scales. Cerebral arterial and aqueductal cerebrospinal fluid (CSF) flow patterns were studied using quantitative phase-contrast angiography. *Results:* Depressed patients had more PVS ( $P < .05$ ) and prolongation of the width of the arterial systolic pulse-wave in the carotid arteries ( $P < .01$ ). There was no significant group difference for any PWV or PWA measurement. TRD patients showed more PVS than other LOD patients ( $P < .05$ ). The fractional width of the arterial systolic peak correlated significantly with augmentation index (AIx) and heart rate-corrected augmentation index (AIx75;  $R^2 = 0.302$ ,  $P < .01$  and  $R^2 = 0.363$ ,  $P < .01$  respectively). Arterial–aqueductal delay showed a negative correlation with estimated aortic systolic pressure (PWVsys;  $R^2 = 0.293$ ;  $P < .01$ ), AIx ( $R^2 = -0.491$ ;  $P < .01$ ) and AIx75 ( $R^2 = -0.310$ ;  $P < .01$ ). PVS scores correlated with AIx ( $R^2 = 0.485$ ;  $P < .01$ ) and AIx75 ( $R^2 = -0.292$ ;  $P < .01$ ). *Conclusion:* Our findings support the hypothesis that increased arterial pulsatility resulting from central arterial stiffness propagates directly into cerebral vessels and is associated with the development of microvascular angiopathy, characterized by dilated PVS and decreased compliance of small arterial vessels.

**Key Words:** Arterial pulsatility—arterial compliance—microvascular angiopathy—treatment-resistant depression

© 2019 Elsevier Inc. All rights reserved.

*Abbreviations:* AAD, arterial-aqueductal delay; AIx, augmentation index; AIx75, heart rate-corrected augmentation index; LOD, late-onset depression; PWA, pulse-wave analysis; PCA, phase-contrast angiography; PVS, perivascular spaces / Virchow-Robin spaces; PWV, aortic pulse-wave velocity; SVD, small vessel disease; TRD, treatment-resistant depression

From the \*Salford Royal NHS Foundation Trust, Salford, United Kingdom; and †Wolfson Molecular Imaging Centre, School of Medicine, University of Manchester, Greater Manchester, United Kingdom.

Received March 29, 2018; revision received December 11, 2018; accepted January 18, 2019.

Funding: No supporting grant.

Address correspondence to Owen M. Thomas, BM, BCh, DPhil, FRCR, Salford Royal NHS Foundation Trust, Stott Lane, Salford M68HD, United Kingdom. E-mail: [Owen.Thomas@srft.nhs.uk](mailto:Owen.Thomas@srft.nhs.uk).

<sup>1</sup>[orcid.org/0000-0003-2877-3075](https://orcid.org/0000-0003-2877-3075).

<sup>2</sup>[orcid.org/0000-0002-3974-0773](https://orcid.org/0000-0002-3974-0773).

<sup>3</sup>[orcid.org/0000-0003-1754-2191](https://orcid.org/0000-0003-1754-2191).

<sup>4</sup>[orcid.org/0000-0002-1623-0383](https://orcid.org/0000-0002-1623-0383).

1052-3057/\$ - see front matter

© 2019 Elsevier Inc. All rights reserved.

<https://doi.org/10.1016/j.jstrokecerebrovasdis.2019.01.020>

## Introduction

Cerebral small vessel disease (SVD) is a common feature of increasing age. It is the commonest cause of vascular dementia and lacunar stroke and has been implicated in cognitive decline and the development of treatment resistant late-onset depression (LOD). A number of imaging biomarkers have been described including the presence of deep white-matter lesions, lacunar infarcts, cerebral microbleeds and dilatation of cerebral perivascular spaces (PVS).<sup>1</sup>

Vascular ageing is also seen in the systemic arterial bed; with increasing age arteries become stiffer and reflected pressure waves return to the central aorta earlier in the cardiac cycle producing augmentation of the systolic pulse wave and of the central arterial systolic pressure. It has been suggested that the development of cerebral SVD might represent a downstream effect of this hemodynamic change. This increase in arterial stiffening has been shown to be associated with cognitive decline.<sup>2-4</sup> Increased arterial stiffening has also been associated with structural changes in the brain, including the presence of white-matter lesions, lacunar infarcts, and cortical atrophy.<sup>5-7</sup> It has also been suggested that increased transmission of systolic pulsations into the brain microvasculature may be the pathogenic mechanism for the development of micro haemorrhages.<sup>8</sup> A recent metareview<sup>9</sup> concluded that higher arterial stiffness is associated with cerebral SVD and white matter hyperintensities in the elderly; and that current findings support the hypothesis that increased pulsations extend through the cerebral arteries into the microcirculation.

In this study, we test the hypotheses that changes in aortic pulse wave produced by arterial stiffening are (1) propagated into cerebral small vessels, (2) associated with reduced compliance of small cerebral arterial vessels, and (3) associated with the presence of dilated PVS. We have used pulse-wave velocity (PWV) and pulse-wave analysis (PWA) to assess peripheral arterial stiffness and direct measurement of cerebral arterial pulse waveforms and cerebral small vessel compliance using quantitative phase-contrast magnetic resonance (MR) imaging.<sup>10</sup>

## Materials and Methods

### Subjects

Patients with LOD were prospectively recruited from secondary care in Greater Manchester. Control subjects were recruited from spouses/partners of patients or by advertisement. The regional ethics committee approved the study. All participants gave full informed consent. Inclusion criteria for patients were: (1) depression consistent with the International Classification of Diseases 10 criteria for a moderate-to-severe depressive episode (with/without psychotic symptoms); (2) age >60 years, and (3) stable medication for >12 weeks. Control subjects were age matched and included on the basis of (1) no

previous history of psychiatric disturbance and (2) stable health. Exclusion criteria were: presence/history of stroke, space occupying lesions, neuro-degenerative disorders/dementia, head injury with loss of consciousness, history of another psychiatric disorder, electroconvulsive treatment within 3 months of recruitment, atrial fibrillation, and severe valvular heart disease.

Resistance to treatment was classified<sup>11</sup> as: (0) response to monotherapy; (1) nonresponse to monotherapy; (2) nonresponse to 2 trials of monotherapy with drugs of different classes; (3) stage 2 plus failure to respond to one augmentation strategy; (4) stage 3 plus failure of a second augmentation strategy; and (5) stage 4 plus failure to respond to 1 course of electroconvulsive treatment. Patients were classified as 'treatment-responsive' (stage 0) and 'treatment-resistant' (stages 1-5).

### General Measures

Age, gender, civil status, smoking status, alcohol intake, medical history (including cardiovascular disease), and medication were recorded. Waist circumference, weight, and height were measured and fasting blood was taken for estimation of glycaemia and lipids. Psychiatric measures included International statistical classification of diseases and related health problems, version 10 (ICD-10) criteria for Depressive Episode, Montgomery Asberg Depression Rating scale for severity<sup>12</sup> and The Mini-Mental Status Examination.<sup>13</sup> Blood pressure (BP) was measured sitting by a semiautomatic machine (Omron 705CP, Omron Medical, Kyoto, Japan) and a mean of 3 readings was recorded.

### Pulse-Wave Velocity (PWV) Measurements

Aortic PWV was determined by Carotid-Femoral Doppler (Micro Medical, Rochester, United Kingdom) using signals from the right carotid and femoral arteries. Ten or more beats were averaged for each site using ECG-gating.<sup>14</sup> Carotid-Femoral PWV was calculated through division of the travelled distance (assessed by tape measure) by the transit time.

### Pulse-Wave (PWA) Analysis

PWA extracts hemodynamic information from the shape of the arterial pressure wave. The central (aortic) pressure waveform is the summation of a forward-going wave generated by left ventricular contraction and a pressure wave reflected back toward the heart from arterial branching points and other sources of impedance mismatch. Arterial stiffening results in an earlier return of the reflected wave in systole, which adds to the forward-going wave to increase the overall systolic pressure (Fig 1). This additional aortic "augmentation pressure" can be measured as the difference between the pressure at the initial systolic shoulder (inflection) and the peak systolic pressure. The "augmentation index" (AIx) is the augmentation pressure expressed as a

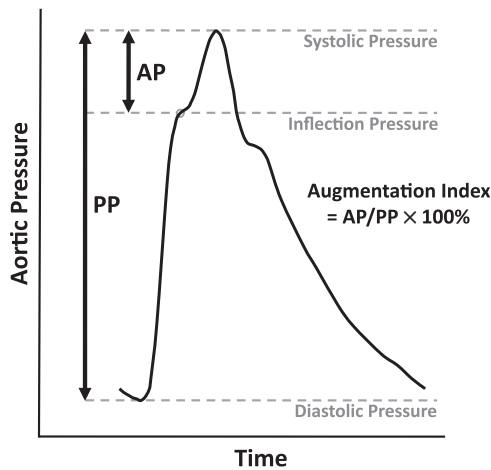


**Figure 1.** Aortic pulse-wave analysis. The aortic pressure waveform is the summation of a forward-going wave (produced by left ventricular contraction) and a pressure wave reflected back from arterial branch points and other regions of impedance mismatch. The reflected wave provides an additional 'augmentation pressure' (AP; measured as systolic pressure–inflection pressure). The 'augmentation index' (AIx) expresses the AP as a fraction of the pulse pressure.

percentage of the pulse pressure (PP), where PP is the difference between the systolic and diastolic BP.<sup>15,16,17</sup>

PWA was performed using a SphygmoCor system (AtCor Medical, Sydney, Australia).<sup>16,17</sup> Peripheral pressure waveforms were acquired from the right radial artery. Several (in theory 20) waveforms were recorded and averaged.<sup>15</sup> The central waveform was derived using a generalised transfer function that then allowed calculation of multiple central indices including AIx, PP, central systolic BP, and time of reflected wave arrival in the aorta. AIx was then normalized to a heart rate of 75.

### Neuroimaging

Subjects were scanned using a 1.5 Tesla Intera Scanner (Philips Medical Systems, Best, Netherlands) using a Birdcage head coil. Anatomical sequences obtained for assessment of deep white matter hyperintensities, lacunar infarction and perivascular space dilatation consisted of (1) 3D volume fluid attenuated inversion recovery (FLAIR); Repetition time (TR)/Echo time (TE)/T1 = 11000/140/2600, section thickness = 3.0 mm and (2) 3D volume T1-weighted inversion recovery (TR/TE/T1 = 6850/18/300). The matrix was 256 × 256, and the field-of-view was 230 × 230 mm.

Measurement of internal carotid and basilar artery blood flow and cerebral aqueduct cerebrospinal fluid (CSF) flow was made with phase-contrast MR angiography (PCA). This technique exploits bipolar gradients (gradients with equal magnitude but opposite directions) to encode velocity: stationary spins will have no net change in phase, while moving spins undergo a phase shift proportional to their velocity. Single-slice PCA was retrospectively ECG-gated with 16 phases for each cardiac cycle. The internal carotid and basilar artery flows were assessed in an oblique-axial plane at the level of the midclivus, above the posterior inferior cerebellar artery origin (Fig 2; slice thickness = 5.0 mm, TR = 12.15 ms, TE = 7.12 ms, image frequency = 64, flip angle = 10, peak velocity encoding value ( $V_{ENC}$ ) = 100 cm s<sup>-1</sup>, phase encoding steps = 192). The cerebral aqueduct was localised on sagittal midline localiser images. Imaging parameters were modified from the arterial sequence (slice thickness = 7.0 mm, TR = 14.95 ms, TE = 9.24 ms,  $V_{ENC}$  = 10 cm s<sup>-1</sup>). Total acquisition time was 45 minutes.

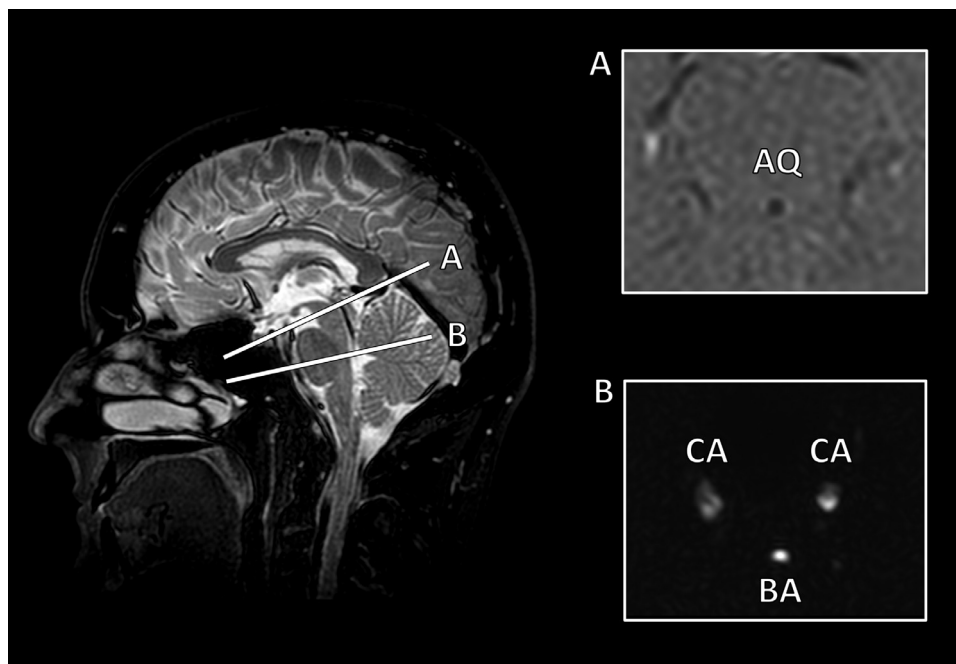


**Figure 2.** Location of the imaging planes for MR phase-contrast angiography (A) cerebral aqueduct (AQ), (B) internal carotid arteries (CA) and basilar artery (BA).

**Table 1.** Description of the derived biomarkers calculated from arterial and aqueductal flow studies<sup>10</sup>

Parameters defining the arterial-CSF flow profile	
aqWSP	The width of the systolic CSF flow peak in the aqueduct—the time period of the systolic (cranio-caudal) CSF flow as a fraction of a cycle, taken from the 0 crossing points
SV	The CSF stroke volume—defined as the average of the systolic and diastolic CSF flow volumes
atWSP	The width of the systolic peak for blood flow in the internal carotid arteries—defined as the narrowest width that corresponds to $0.7 \times$ (total area under the curve); this should correspond to approximately the width at half height.
AAD	The arterial-aqueductal delay—defined as the time between the centre of the arterial peak and the centre of the aqueduct peak.

### Image Analysis

PCA MRI images were analysed using freely available software, SEGMENT.<sup>18</sup> A region of interest was manually defined for each artery and the cerebral aqueduct. These were then applied to each frame of the cardiac cycle. The user was blinded to the depression/control status.

The Arterial-Aqueductal Flow Data Analysis Tool (Copyright (c)2006, Translational Imaging Unit, University of Manchester, United Kingdom<sup>10</sup>) was used to generate further flow indices (Table 1; Fig 3).

White-matter lesions were assessed using a previously validated modified Sheltens score.<sup>19,20</sup> The independent scoring of putamen and globus pallidus was replaced with a composite score for the lentiform nucleus on the basis of poor reproducibility and inter-rater agreement. Axial T1 inversion recovery images were used for PVS scoring.<sup>21,22</sup> Two previously described scoring systems were used, the first designed to quantify PVS when disease load is low and the second designed for use where PVS are numerous<sup>21,22</sup> (Fig 4).

### Statistical Analysis

Statistical analyses were performed in SPSS v22.0 (IBM) and In-Stat (Graph pad, San Diego, California). Group-wise comparisons were performed comparing control subjects to depressed patients using chi-squared tests for contingency tables for categorical variables and z-scores for numeric variables. Correlations between PWA and PWV parameters and imaging features were performed using a Fisher z-transformation. Probability thresholds were set at 5% but the Šidák correction for multiple tests was applied in all cases.

### Results

A total of 34 subjects were recruited, 15 normal volunteers and 19 patients with LOD. Demographic and basic clinical data is shown in Table 2. There were no significant differences in age for gender between the groups. Single status was commoner in LOD than in controls ( $P < .5$ ), High alcohol

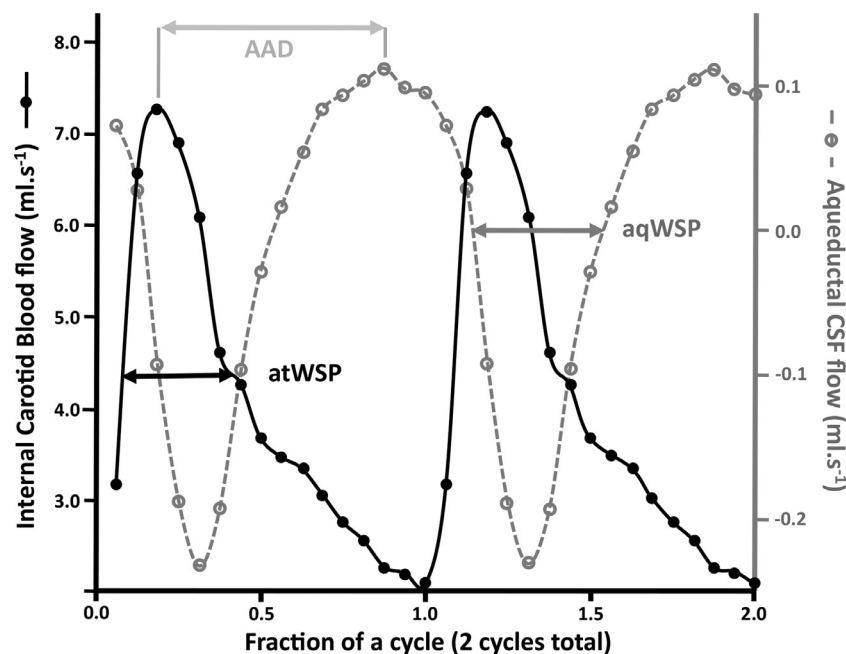


**Figure 3.** Example of PC-MRI measured (A) internal carotid artery blood flow (left-hand ordinate scale) and (B) aqueductal CSF flow (right-hand ordinate scale). Width of the systolic peak in the internal carotid arteries (atSWP), width of the systolic peak in the cerebral aqueduct (aqSWP) and arterial-aqueductal delay (AAD) are as defined in Table 1.

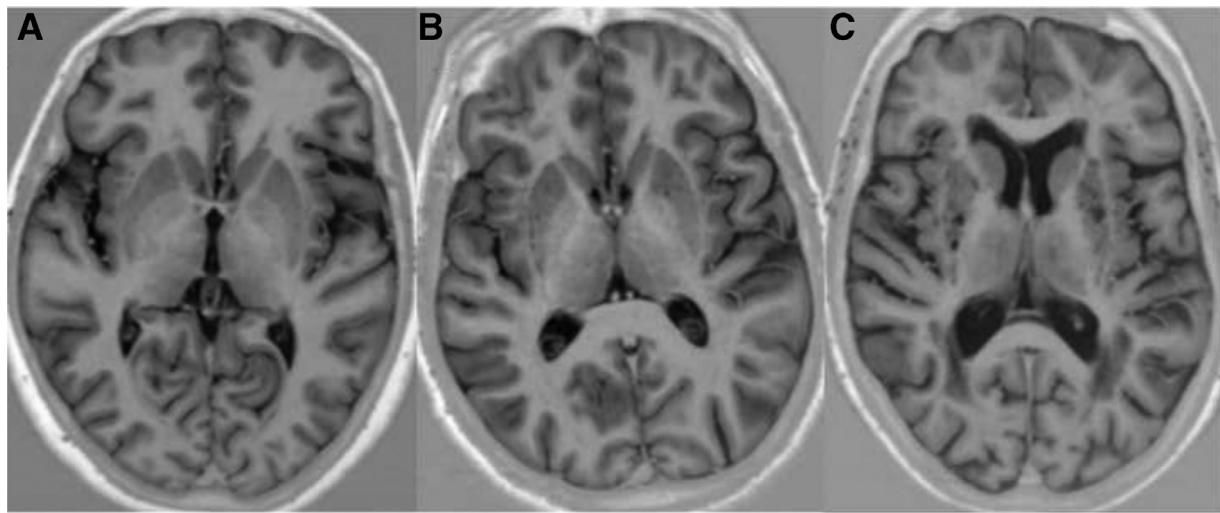


**Figure 4.** Axial T1 inversion recovery images illustrating the spectrum of PVS disease load. Two PVS scoring schemes were used.<sup>21,22</sup> (A) minimal burden (scores 0 and 1); (B) mild burden (4 and 3); and (C) severe burden (7 and 6).

**Table 2.** Demographic and basic clinical data for all subjects

Variable	Demographics of study sample		
	All subjects (n = 34)	Depressed (n = 19)	Controls (n = 15)
Age, y (mean)	72.26	72.21	72.33
Women, n	23	13	10
Married, n	17	5	12*
Ethnicity-European, n	32	18	14
Alcohol units/wk	5.50	4.05	7.33*
Smoking status, n	10.00	4.00	6.00
Smoking pack years	13.74	13.95	13.47
Diabetes, n	2	1	1
Statin use, n	12	9	3
Body mass index, kg/m <sup>2</sup>	28.71	28.43	29.05
Waist circumference, cm	97.42	97.31	97.68
Systolic blood pressure, mmHg	142	140	146
Diastolic blood pressure, mmHg	76.91	76.53	77.40
Total cholesterol, mmol/l	4.81	4.85	4.76
HDL, mmol/L	1.49	1.53	1.44
TG, mmol/L	1.34	1.33	1.36
Glucose, mmol/L	5.40	5.16	5.69

Abbreviations: HDL, high density lipoprotein; TG, triglycerides.

Significant differences between depressed in control subjects are indicated by \*( $P < .05$ ).

consumption was commoner in controls than in LOD ( $P < .05$ ) no other differences reached statistical significance.

Of the 19 patients with depression, 6 fulfilled the criteria for treatment-resistant depression (TRD). Demographic and basic clinical data for late onset depression and TRD are shown in Table 3. Alcohol intake was significantly higher in TRD patients. No other significant differences were seen between the groups.

Table 4 shows the values of representative MR imaging, PWV, and PWA biomarkers for each of the groups. Depressed patients had significantly higher basal ganglia perivascular space dilatation ( $P < .05$ ) and also showed relative prolongation of the width of the arterial systolic

pulse wave in the carotid arteries ( $P < .01$ ). There was no significant difference between groups for any PWV or PWA measurement. TRD patients showed significantly higher basal ganglia perivascular space dilatation than LOD patients ( $P < .05$ ) and basal ganglia PVS scores of 4 and 5 were seen only in the TRD group.

Fractional width of the arterial systolic peak correlated significantly with AIX and AIX75 ( $R^2 = 0.302$ ;  $P < .01$  and  $R^2 = 0.363$ ;  $P < .01$  respectively). Arterial-aqueductal delay (AAD) showed a negative correlation with estimated aortic systolic pressure (PWVsys;  $R^2 = -0.293$ ;  $P < .01$ ); AIX ( $R^2 = -0.491$ ;  $P < .01$ ) and heart-rate normalized AIX75 ( $R^2 = -0.310$ ;  $P < .01$ ). There was no correlation between

**Table 3.** Demographic and basic clinical data for all subjects showing separate results for subjects with treatment-resistant depression (TRD) and non-treatment resistant late-onset depression (LOD)

Variable	Demographics of study sample		
	All subjects (n = 19)	LOD (n = 13)	TRD (n = 6)
Age, y (mean)	72.21	72.15	72.33
Women, n	13	9	4
Married, n	5	3	2
Ethnicity-European, n	18	12	6
Alcohol units/wk	4.05	1.23	10.17*
Smoking status, n	6	4	2
Smoking pack years	13.47	11.10	20.00
Diabetes, n	1	1	0
Statin use, n	9	5	4
Body mass index, kg/m <sup>2</sup>	28.43	28.52	28.24
Waist circumference, cm	97.31	97.16	97.64
Systolic blood pressure, mmHg	140	142	136
Diastolic blood pressure, mmHg	77	75	79
Total cholesterol, mmol/L	4.85	5.05	4.41
HDL, mmol/L	1.53	1.57	1.42
TG, mmol/L	1.33	1.22	1.55
Glucose, mmol/L	5.16	5.07	5.35

Significant differences between LOD and TRV groups are indicated by \* ( $P < .05$ ).

**Table 4.** Median values for imaging biomarkers and for pulse-wave velocity and pulse-wave analysis derived parameters

Variable	MR biomarker distribution			
	Controls (n = 15)	Depressed (n = 19)	LOD (n = 13)	TRD (n = 6)
Total Scheltens score	11.25	8.79	8.54	9.33
Periventricular WMH score	1.94	2.10	1.92	2.5
Deep WMH score	6.43	5.52	5.62	5.33
Basal ganglia PVS score	2.68	3.72*	3.33	4.5*
Deep white matter PVS score	0.93	1.06	1.28	0.67
aqWSP (%)	0.45	0.46	0.47	0.45
AAD (%)	0.19	0.18	0.17	0.16
atWSP (%)	0.29	0.33**	0.33	0.32
aqSys V	53.3	53.3	53.8	52.2
Variable	PWV and PWA biomarker distribution			
	Controls (n = 15)	Depressed (n = 19)	LOD (n = 13)	TRD (n = 6)
PWV <sub>sp</sub>	146.0	140.8	143.0	136.0
PWV <sub>dp</sub>	77.4	76.4	75.39	78.67
PWV	10.11	11.57	11.54	11.83
AP	21.1	20.1	21.85	16.5
AIx	33.67	34.78	37.15	26.67

Abbreviations: AAD, arterial-aqueductal delay; AIx, augmentation index; AP, augmentation pressure; LOD, late-onset depression; PWA, pulse-wave analysis; PWV, pulse-wave velocity; PVS, perivascular spaces; TRD, treatment-resistant depression; WMH, white matter hyperintensity.

Significant differences between controls and depressed groups are indicated in the second column (Depressed), significant differences between LOD and TRD are shown in the fourth column (TRD). Significance levels are indicated by \* ( $P < .05$ ) or \*\* ( $P < .01$ ).

CSF flow parameters and any other imaging biomarker. Severity of basal ganglia perivascular space dilatation demonstrated significant correlation with AIx ( $R^2 = 0.485$ ;

$P < .01$ ) and AIx75 ( $R^2 = -0.292$ ;  $P < .01$ ). No other imaging biomarkers correlated with any PWV or PWA derived parameters.

## Discussion

Arterial stiffening is a hallmark of increasing age and reflects structural changes within vessel walls. As the compliance of peripheral arterial vessels decreases, the speed of arterial wave propagation increases so that reflected pressure waves arrive back in the aorta during systole rather than diastole. Increased pulse wave reflection results in increased systolic pressure, high resting flow and increased pulsatility into the vascular tree.<sup>9</sup> Several groups have hypothesized that increased pulsatility propagates through the carotid and vertebral arteries and extends into the brain microvasculature resulting in worsening of SVD with consequent increases in white-matter lesions, lacunar infarcts cerebral micro-hemorrhage and cerebral atrophy.<sup>5-7</sup> One recent review<sup>9</sup> concluded that

“higher arterial stiffness is associated with cerebral SVD and white matter hyperintensities in the elderly; and that current findings support the hypothesis that increased

pulsations extend through the cerebral arteries into the microcirculation.”

However, the authors stress that no causative link has been proven and that the relationship between SVD and arterial stiffness may be indirect, perhaps reflecting shared vascular risk factors. In the current study we have shown strong correlation between the AIx and the fractional width of the arterial systolic peak. This confirms the suggestion of previous groups that increased pulsatility is propagated into the major cerebral arteries.

In recent years, there has been growing interest in imaging biomarkers of SVD and, in particular of the relationship between dilated PVS and the presence of SVD.<sup>1</sup> Dilatation of PVS surrounding the penetrating arteries and arterioles, particularly in the striothalamic vessels, has been shown to provide a more specific biomarker than deep white matter hyperintensities in a number of conditions strongly associated with cerebral microangiopathy. These include distinction between normal subjects with high and low vascular

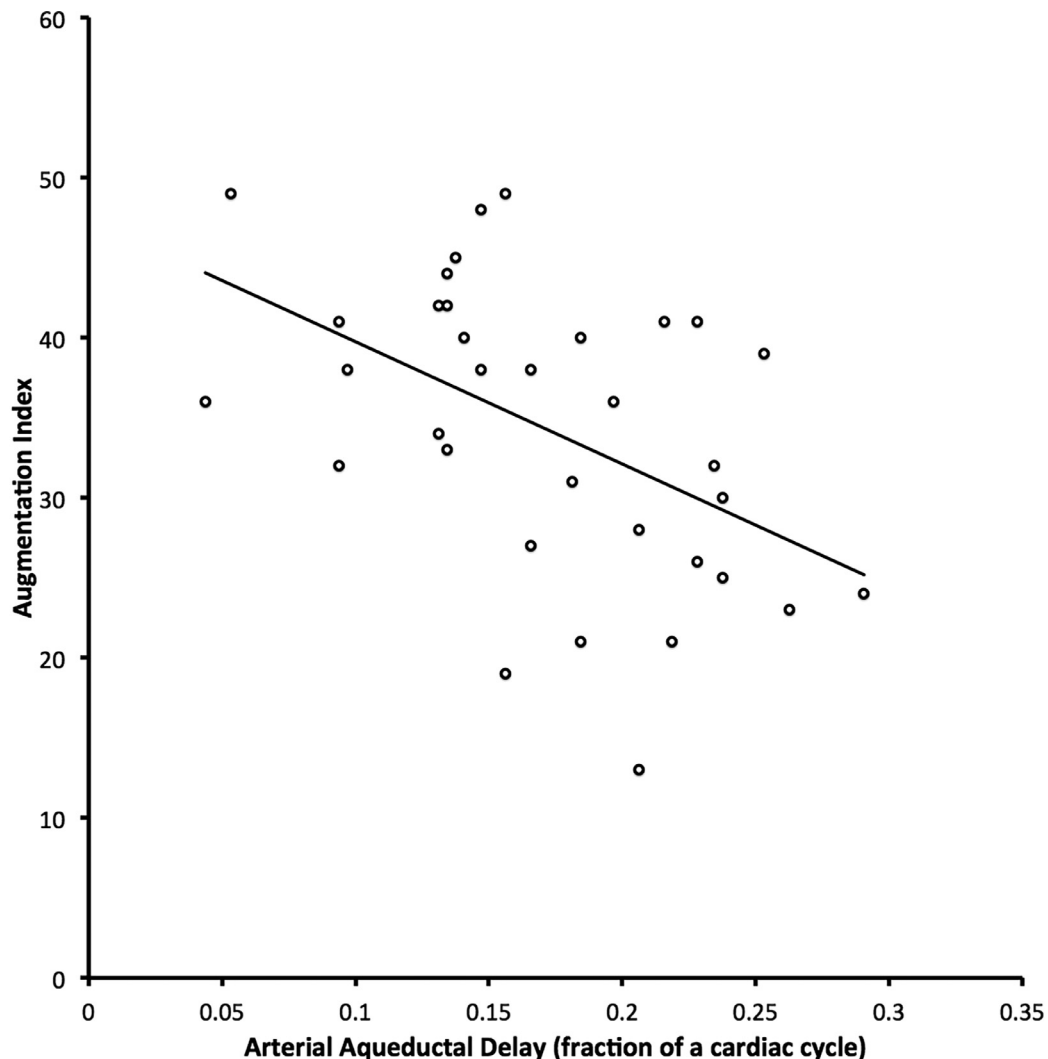


Figure 5. Relationship between arterial-aqueeductal delay (AAD) and peripheral augmentation index (AIx).

risk factors,<sup>23</sup> separation between vascular and neurodegenerative dementias<sup>20,21</sup> and identification of treatment resistant subgroups in patients with late onset depression.<sup>22,24</sup> It has been hypothesized that dilated PVS are a direct biomarker of small arterial vessel disease, as demonstrated by histopathology,<sup>21</sup> while white-matter lesions can result from a number of other pathogenetic mechanisms.

In the current study, we have demonstrated the previously reported relationship between TRD and increased PVS in the basal ganglia.<sup>24</sup> More importantly, we have shown that PVS dilatation is associated with increasing pulse wave augmentation. These findings support the hypothesis that increased arterial pulsatility resulting from increasing peripheral arterial stiffness are directly associated with the development of microvascular angiopathy. We did not observe a statistically significant relationship between PWV or AIx and white matter hyperintensity scores. Such a link has been described by one previous study<sup>25</sup> although another found increased baseline arterial stiffness to be associated only with increases in the volume of hyperintensity in the left superior longitudinal fasciculus at follow-up.<sup>26</sup>

The use of cerebral PWA using quantitative PCA has been applied in a number of studies examining the role of cerebral SVD. The development of decreased compliance in small arterial cerebral vessels due to microvascular angiography has been shown to result in more rapid passage of the systolic pressure wave from the arterial vessels to CSF (AAD). We have shown a significant negative correlation between AAD and estimated aortic systolic pressure (PWVsys;  $P < .01$ ); AIx ( $R^2 = -0.491$ ;  $P < .01$ ) and AIx75 ( $R^2 = -0.310$ ;  $P < .01$ ; Fig 5). These findings again are entirely in keeping with the hypothesis that microvascular angiography, characterized by decreased small arterial vessel compliance in the brain, is associated with peripheral arterial stiffness.

One weakness of the study is the relatively small size of the study population although statistical comparisons were all corrected for type I statistical errors. Another major weakness is that we do not have follow-up data on these subjects to examine the hypothesis that increased arterial stiffness is associated with development of microvascular angiopathy.

## Conclusions

Overall, our findings provide evidence to support the hypothesis that an increase in arterial pulsatility resulting from central arterial stiffness propagates directly into cerebral vessels and that this is directly associated with the development of microvascular angiopathy, characterized by the development of dilated PVS and decreased compliance of small arterial vessels.

## References

1. Wardlaw JM, Smith EE, Biessels GJ, et al. Neuroimaging standards for research into small vessel disease and its contribution to ageing and neurodegeneration. *Lancet Neurol* 2013;12:822-838.
2. Elias MF, Robbins MA, Budge MM, et al. Arterial pulse wave velocity and cognition with advancing age. *Hypertension* 2009;53:668-673.
3. Tarumi T, Gonzales MM, Fallow B, et al. Central artery stiffness, neuropsychological function, and cerebral perfusion in sedentary and endurance-trained middle-aged adults. *J Hypertens* 2013;31:2400-2409.
4. Singer J, Trollor JN, Crawford J, et al. The association between pulse wave velocity and cognitive function: the Sydney Memory and ageing study. *PLoS One* 2013;8:e61855.
5. Henry-Feugeas MC, Roy C, Baron G, et al. Leukoaraiosis and pulse-wave encephalopathy: observations with phase-contrast MRI in mild cognitive impairment. *J Neuroradiol* 2009;36:212-218.
6. Kim CK, Lee SH, Kim BJ, et al. Age-independent association of pulse pressure with cerebral white matter lesions in asymptomatic elderly individuals. *J Hypertens* 2011; 29:325-329.
7. Saji N, Shimizu H, Kawarai T, et al. Increased brachial-ankle pulse wave velocity is independently associated with white matter hyperintensities. *Neuroepidemiology* 2011;36:252-257.
8. Henskens LH, van Oostenbrugge RJ, Kroon AA, et al. Brain microbleeds are associated with ambulatory blood pressure levels in a hypertensive population. *Hypertension* 2008; 51:62-68.
9. Singer J, Trollor JN, Baune BT, et al. Arterial stiffness, the brain and cognition: a systematic review. *Ageing Res Rev* 2014;15:16-27.
10. Naish JH, Baldwin RC, Patankar T, et al. Abnormalities of CSF flow patterns in the cerebral aqueduct in treatment-resistant late-life depression: a potential biomarker of microvascular angiopathy. *Magn Reson Med* 2006; 56:509-516.
11. Thase ME. Management of patients with treatment-resistant depression. *J Clin Psychiatry* 2008;69:e8.
12. Montgomery SA, Asberg M. A new depression scale designed to be sensitive to change. *Br J Psychiatry* 1979; 134:382-389.
13. Folstein MF, Folstein SE, McHugh PR. "Mini-mental state". A practical method for grading the cognitive state of patients for the clinician. *J Psychiatr Res* 1975; 12:189-198.
14. Baguet JP, Kingwell BA, Dart AL, et al. Analysis of the regional pulse wave velocity by Doppler: methodology and reproducibility. *J Hum Hypertens* 2003;17:407-412.
15. Wilkinson IB, Fuchs SA, Jansen IM, et al. Reproducibility of pulse wave velocity and augmentation index measured by pulse wave analysis. *J Hypertens* 1998; 16:2079-2084.
16. O'Rourke MF, Pauca A, Jiang XJ. Pulse wave analysis. *Br J Clin Pharmacol* 2001;51:507-522.
17. Laurent S, Cockcroft J, Van Bortel L, et al. Expert consensus document on arterial stiffness: methodological issues and clinical applications. *Eur Heart J* 2006;27:2588-2605.
18. Heiberg E, Sjögren J, Ugander M, et al. Design and validation of segment—a freely available software for cardiovascular image analysis. *BMC Med Imaging* 2010;10:1.
19. Scheltens P, Barkhof F, Valk J, et al. White matter lesions on magnetic resonance imaging in clinically diagnosed Alzheimer's disease. Evidence for heterogeneity. *Brain* 1992;115:735-748.

20. Hansen TP, Cain J, Thomas O, et al. Dilated perivascular spaces in the Basal Ganglia are a biomarker of small-vessel disease in a very elderly population with dementia. *AJNR Am J Neuroradiol* 2015;36:893-898.
21. Patankar TF, Mitra D, Varma A, et al. Dilatation of the Virchow-Robin space is a sensitive indicator of cerebral microvascular disease: study in elderly patients with dementia. *AJNR Am J Neuroradiol* 2005;26:1512-1520.
22. Doubal FN, MacLulich AM, Ferguson KJ, et al. Enlarged perivascular spaces on MRI are a feature of cerebral small vessel disease. *Stroke* 2010;41:450-454.
23. Selvarajah J, Scott M, Stivaros S, et al. Potential surrogate markers of cerebral microvascular angiopathy in asymptomatic subjects at risk of stroke. *Eur Radiol* 2009;19:1011-1018.
24. Patankar TF, Baldwin R, Mitra D, et al. Virchow-Robin space dilatation may predict resistance to antidepressant monotherapy in elderly patients with depression. *J Affect Disord* 2007;97:265-270.
25. King KS, Chen KX, Hulsey KM, et al. White matter hyperintensities: use of aortic arch pulse wave velocity to predict volume independent of other cardiovascular risk factors. *Radiology* 2013;267:709-717.
26. Rosano C, Watson N, Chang Y, et al. Aortic pulse wave velocity predicts focal white matter hyperintensities in a biracial cohort of older adults. *Hypertension* 2013;61:160-165.